Wesley, Reading, Mass., 1977); W. K. Pratt, *Digital Imaging Processing* (Wiley, New York, 1978).
39. W. T. Cathey, B. R. Frieden, W. T. Rhodes, C. K. Rushforth, *J. Opt. Soc. Am. A* **3**, 241 (1984).
40. M. J. B. Duff, Ed. *Computing Structures for Image Processing* (Academic Press, London, 1983); D. A. Symanow, D. J. Svetkoff, P. F. Leonard, *Electronic Imaging*, 46 (February, 1985). On the Delft image analysis laboratory system, see F. A. Gerritsen, thesis, Technical University of Delft, Delft, Netherlands (1982); R. P. W. Duin, in *Computing Structures for Image Processing*, M. J. B. Duff, Ed. (Academic Press, London, 1983), p. 141.
41. S. J. Kaufman *et al.*, *Exp. Cell Res.* **25**, 333 (1980); K. R. Haye, R. F. Foster, S. J. Kaufman, *J. Cell Biol.* **99**, 312a (1984); S. J. Kaufman and R. Robert-Nicoud, *Cytometry*, in press.
42. F. S. Fay and C. M. Delise, *Proc. Natl. Acad. Sci. U.S.A.* **70**, 641 (1973).
43. D. Axelrod, D. E. Koppel, J. Schlessinger, E. L. Elson, W. W. Webb, *Biophys. J.* **16**, 1055 (1976); D. E. Koppel, *ibid.* **28**, 281 (1979); G. M. McGregor, H. G. Kapitza, K. A. Jacobsen, *Laser Focus*, 85 (November 1984); H. G. Kapitza, G. McGregor, K. A. Jacobsen, *Proc. Natl. Acad. Sci. U.S.A.* **82**, 4122 (1985).
44. B. M. Salzberg, in *Current Methods in Cellular Neurobiology*, J. L. Barker, Ed. (Wiley, New York, 1983), p. 139; A. Grinvald, *Annu. Rev. Neurosci.* **8**, 263 (1985).
45. T. M. Jovin *et al.*, *Cold Spring Harbor Symp. Quant. Biol.* **47**, 143 (1983); D. A. Zarling, D. J. Arndt-Jovin, M. Robert-Nicoud, R. Thomae, L. P. McIntosh, T. M. Jovin, *J. Mol. Biol.* **176**, 369 (1984); D. J. Arndt-Jovin, M. Robert-Nicoud, D. A. Zarling, C. Greider, E. Weimer, T. M. Jovin, *Proc. Natl. Acad. Sci. U.S.A.* **80**, 4344 (1983).
46. D. J. Arndt-Jovin, M. Robert-Nicoud, P. Baurschmidt, T. M. Jovin, *J. Cell Biol.*, in press.
47. F. S. Fay, R. T. Fujiwara, K. Fogarty, D. J. Rees, *Cell Biol.* **96**, 783 (1983); F. S. Fay, K. E. Fogarty, J. M. Coggins, in *Optical Methods in Cell Physiology*, P. DeWeer and B. Salzburg, Eds. (Wiley, New York, in press).
48. D. A. Agard and J. W. Sedat, *Nature (London)* **302**, 676 (1983); D. Mathog, M. Hochstrasser, J. W. Sedat, *J. Microsc.* **137**, 241 (1985).
49. D. Mathog, M. Hochstrasser, Y. Gruenbaum, H. Saumweber, J. Sedat, *Nature (London)* **308**, 414 (1984); Y. Gruenbaum, M. Hochstrasser, D. Mathog, H. Saumweber, D. A. Agard, J. W. Sedat, *J. Cell Sci. Suppl.* **1**, 223 (1984); D. Mathog, *J. Microsc.* **137**, 253 (1985); M. Hochstrasser, D. Mathog, Y. Gruenbaum, H. Saumweber, J. W. Sedat, *J. Cell. Biol.*, in press.
50. H.-G. Keyl, *Chromosoma* **8**, 739 (1957).
51. The references to actual or proposed implementation with digital and other image processing techniques are deemed to be representative and current but do not constitute a comprehensive survey of the relevant literature.
52. H. Piller, *Microscope Photometry* (Springer, Berlin, 1977).
53. R. D. Allen, J. L. Travis, N. S. Allen, H. Yilmay, *Cell Motility* **1**, 275 (1981); R. J. Walter and M. W. Berns, *Proc. Natl. Acad. Sci. U.S.A.* **78**, 6927 (1981); K. Yamamoto and A. Taira, *J. Microsc.* **129**, 49 (1983).
54. R. D. Allen and N. S. Allen, *J. Microsc.* **129**, 3 (1983).
55. J. S. Ploem, *Z. Wiss. Mikr.* **68**, 129 (1967).
56. J. A. Dvorak, L. H. Miller, W. C. Whitehouse, T. Shiroishi, *Science* **187**, 748 (1975); R. D. Allen, N. S. Allen, J. L. Travis, *Cell Motility* **1**, 291 (1981); S. Inoue, *J. Cell Biol.* **89**, 346 (1981); K. R. Spring, *Pfluegers Arch.*, in press.
57. D. Keller, C. Bustamante, M. F. Maestre, I. Tinoco, Jr., *Proc. Natl. Acad. Sci. U.S.A.* **82**, 401 (1985).
58. W. Mickols, J. E. Katz, M. F. Maestre, I. Tinoco, Jr., C. Bustamante, *Rev. Sci. Instrum.*, in press; W. Mickols, M. F. Maestre, I. Tinoco, Jr., S. H. Embury, *Proc. Natl. Acad. Sci. U.S.A.*, in press.
59. B. Kachar, *Science* **227**, 766 (1985); *ibid.*, p. 1355; C. J. R. Sheppard and D. K. Hamilton, *Appl. Optics* **22**, 886 (1983).
60. D. Axelrod, *Cell Biophys.* **3**, 167 (1981); R. N. Smartt and W. H. Steel, *Appl. Opt.* **24**, 1402 (1985).
61. G. W. Ellis, in *ICN–UCLA Symposium on Molecular and Cellular Biology*, E. R. Dirksen, D. M. Prescott, C. F. Fox, Eds. (Academic Press, New York, 1978), vol. 12, p. 465.
62. C. J. R. Sheppard and R. Kompfner, *Appl. Opt.* **17**, 2879 (1978); see also (*15*).
63. G. T. Reynolds, *Q. Rev. Biophys.* **5**, 295 (1972); I. Pastan, W. W. Webb, E. L. Elson, *Proc. Natl. Acad. Sci. U.S.A.* **74**, 2909 (1977); J. Schlessinger, Y. Schechter, M. Willingham, I. Pastan, *ibid.* **75**, 2659 (1978).
64. J. W. MacInnes and R. B. Uretz, *Science* **151**, 689 (1966); G. V. Sengbusch and A. Thaer, in *Fluorescence Techniques in Cell Biology*, A. A. Thaer and M. Sernetz, Eds. (Springer, Berlin, 1973), p. 31; T. M. Jovin, in *Flow Cytometry*, M. Melamed, P. Mullaney, M. Mendelsohn, Eds. (Wiley, New York, 1979), p. 137; J. E. Solomen, *Appl. Opt.* **20**, 1537 (1981).
65. S. M. Fermandez and R. D. Berlin, *Nature (London)* **264**, 411 (1976); L. Trón *et al.*, *Biophys. J.* **45**, 939 (1984).
66. D. J. Arndt-Jovin, S. A. Latt, G. Striker, T. M. Jovin, *J. Histochem. Cytochem.* **27**, 87 (1979).
67. T. Hirschfeld, *Can. J. Spectrosc.* **10**, 128 (1965); D. Axelrod, *J. Cell Biol.* **89**, 141 (1981); D. Axelrod, T. P. Burghardt, N. L. Thompson, *Annu. Rev. Biophys. Bioeng.* **13**, 247 (1984); F. Lanni, A. S. Waggoner, D. L. Taylor, *J. Cell Biol.* **100**, 1091 (1985).
68. P. Johnson and P. B. Garland, *FEBS Lett.* **132**, 252 (1981); *Biochem. J.* **203**, 313 (1982).

69. We thank K. Spring for helpful discussions and assistance with reference material; F. S. Fay, J. W. Sedat, and M. Nederlof for providing data and figures included in this article; I. T. Young for helpful discussions and collaborations; H. Epelbaum for assistance in producing the figures; and V. Wilke and the Carl Zeiss Company for the loan of a prototype laser scan microscope. Supported by the Max Planck Society and the German Research Council. S. J. Kaufman was supported as a Senior International Fellow by grant FO6 TWOO960 from the Fogarty International Center of the National Institutes of Health. T. M. Jovin was a Fogarty Scholar-in-Residence at NIH during the compilation of this manuscript.

---

# Time-Resolved Electron Energy Loss Spectroscopy

T. H. Ellis, L. H. Dubois, S. D. Kevan, M. J. Cardillo

In the past two decades, powerful techniques have been developed to study in detail the static properties of simple, well-defined surfaces. A good foundation is now being laid in understanding surface geometries, electronic structures, and vibrational frequencies (*1–3*). The elucidation of elementary surface rate processes is a more complex endeavor, however, and less progress has been made toward this goal (*4–6*). Despite the fact that numerous technologically important processes such as electronic materials growth and processing, heterogeneous catalysis, and corrosion are governed by surface kinetics, a suitable surface probe of rate processes that possesses sufficient dynamic range and chemical sensitivity to yield useful kinetic information has not yet been developed.

Two recent developments in the experimental technique of electron energy–loss spectroscopy (EELS)—dispersion compensation (*7*) and parallel detection (*8*)—have led to the measurement of surface vibrational spectra with a signal strength several orders of magnitude higher than the strength in conventional systems. This increased signal strength permits the measurement of the rates of surface processes on the millisecond time scale, thereby making possible time-resolved EELS (TREELS).

The exploitation of TREELS will significantly expand the capabilities of both thermal desorption spectroscopy and molecular-beam surface scattering. These latter techniques have provided useful kinetic information in the past (*4–6*), but they have been limited to detection of gas-phase products only (that is, they observe the final result of a series of elementary reaction steps on the surface rather than the individual steps themselves).

While the possibilities presented by TREELS are as broad as chemistry itself, four of them have special relevance to both fundamental and applied research:

1) Time-resolved adsorption studies can measure the dynamic properties of metastable precursor and nonequilibrium adsorption states, as well as the dependence of the sticking probability on the incident particle and substrate properties (*9–12*). In addition, sensitive, time-resolved studies will allow investi-

---

T. H. Ellis is a Natural Sciences and Engineering Research Council of Canada postdoctoral fellow, L. H. Dubois is a member of the technical staff in the Physical and Inorganic Chemistry Department, S. D. Kevan is a member of the technical staff in the Condensed State Physics Department, and M. J. Cardillo is head of the Chemical Physics Department, AT&T Bell Laboratories, Murray Hill, New Jersey 07974.

gations of the pervasive effects of defects and adsorbate interactions encountered in the adsorbed state and in the desorption process leading to kinetic nonlinearities and compensation effects associated with phase transitions (*13, 14*).

2) Studies of unimolecular decomposition have been fundamental in establishing, in the gas phase, the nature of intramolecular energy flow and of bond-breaking in chemical events (*15, 16*). Such studies will likely play a comparable role in establishing the nature of these processes on surfaces. The goal is to characterize the various decomposition pathways by identifying transient intermediates and measuring their lifetimes.

3) A real-time characterization of simple reactive events between adsorbed species can provide a wealth of fundamental information concerning the role of transient species and elementary reaction pathways on a surface. It will be possible to investigate the effect on such reactions of surface topography, defects, promoters and inhibitors, and composition.

4) The fundamental processes underlying the growth of crystals and materials involve both surface diffusion and the kinetics of bond-breaking or bond-forming (*17–20*). The details of these processes are virtually unknown and underlie a variety of technologically important processes.

Any surface process can be separated into three generic steps (*5*): (i) adsorption of reactants from the gaseous ambient, (ii) reaction on the surface, and (iii) desorption of the products. The principal benefit of TREELS is to allow investigators to obtain a detailed, fundamental understanding of the reaction pathways and rates involved in the second step. To attain this understanding, it is essential to control and monitor the other two steps as well. This leads to the natural coupling of time-resolved surface spectroscopy both to a molecular beam, for preparing well-defined reactants, and to either a mass spectrometer or laser, for monitoring products. Although several experimental configurations are possible, we use the molecular beam to define the temporal waveform of the reactants. The rate processes on the surface alter the waveforms of adsorbates, surface intermediates, and products, and these altered waveforms are then detected by EELS. Analysis of the TREELS data using suitable theoretical models yields the desired surface kinetic information. The desorption distributions detected with a laser or mass spectrometer complete the description of the surface chemistry.

*Summary.* Two recent instrumental improvements in high-resolution electron energy loss spectroscopy make possible the recording of complete surface vibrational spectra on the millisecond time scale. This is the first spectroscopic probe capable of directly measuring fundamental surface rate processes in real time with a resolution less than or equal to 1 millisecond. Such measurements are the key to understanding surface kinetics at the molecular level. This article summarizes experiments on the adsorption and decomposition of formic acid on Cu(100) to investigate the temperature and coverage dependence of the formate intermediate. Other results are cited that provide a detailed description of the decomposition of methanol on Ni(110). Also reported are direct measurements of the residence time of carbon monoxide on Cu(100) and the associated desorption kinetics.

The choice of EELS to monitor the second step is dictated by both its high signal-to-noise level and the intrinsic chemical sensitivity of vibrational spectroscopy (*3*). Standard EELS spectrometers yield adequate spectra after signal averaging for 1 to 3 seconds at a single loss frequency. The instruments used in TREELS studies improve on this by about two orders of magnitude (*7, 8*). An achievable time resolution in all three experimental steps (adsorption, surface reaction, and desorption) is thus of the order of milliseconds. Attainment of such resolution will open to study, for example, the regime of activated surface processes.

Although in principle a specific activated process can be examined on any given time scale by simply choosing an appropriate temperature, a dynamic process is rarely dominated by one kinetic event over a rate change of several orders of magnitude. A typical rate process consists of many elementary dynamic steps, each of which may have different temperature and concentration dependences. As the time domain of the measurement is shortened, the various fundamental components of the rate process are revealed. The long-time resolution limit is imposed by sample and spectrometer stability. Thus, the time range achieved in the TREELS instruments discussed here, 1 millisecond to 1 hour, represents the first stage in characterizing those processes that underlie surface chemistry.

## EELS Instrumentation

The EELS experiment is qualitatively similar to a Raman light-scattering experiment (*21*). In both techniques, as monochromatic a beam of particles as possible (electrons in EELS and photons in Raman) is produced and scattered off a sample. The energy of the scattered beam is then analyzed to differentiate between the particles that have been elastically scattered and those that have excited a vibrational mode of the sample.

The standard EELS spectrometer operates in a serial fashion (*3*). Electrons from a hot cathode are made monochromatic by an electrostatic deflector, imaged to and from the sample by electrostatic lenses, analyzed by a second deflector, and finally detected individually with an electron multiplier (Fig. 1a). A spectrum is recorded by varying the analyzer energy relative to that of the monochromator.

As in a Raman experiment, the most obvious way to increase signal strength in such experiments is to introduce parallel processing. One way to do that is to use parallel detection of electron energies with a position-sensitive detector located at the exit plane of the analyzer. Signal strength is increased in direct proportion to the total energy range detected. This procedure, currently popular in other electron spectroscopies (*22, 23*), has recently been introduced into EELS instrumentation (*8*). Results obtained with this design will be presented in the next section.

A more subtle parallel-processing technique, which is generally inapplicable to Raman spectroscopy, makes use of the parallel scattering of electrons off the sample over a range of energies (*7*). Because of the inherent limitations of space-charge effects in electrostatic monochromators, the signal enhancement achieved with this technique will have a greater than linear functional dependence on the energy spread of the scattered electrons (*3*). The potential exists for achieving signal enhancements at least two orders of magnitude better than can be obtained with standard designs. In addition, these two types of parallel processing are not mutually exclusive, and they will be combined in new, more advanced machines.

The technique used to achieve scattering at parallel incident energies, called dispersion compensation, has been described in detail (*7*). To understand how it works, one must first recall that electrostatic deflection analyzers operate by converting a spread in electron energies at the entrance slit to a spread in space at the exit plane (like light passing through a prism). Figure 1a shows how conventional EELS uses this property. A slit placed at the exit plane of the monochromator serves to select a narrow energy distribution from the broad energy spread at the filament.

When the electrons scatter from the surface, a new energy spread is created, and this is the electron energy loss spectrum that is to be measured. The analyzer disperses this energy distribution across its exit plane. The spectrum is then measured by sweeping the energy distribution across a single slit and detector. The improvement made by Ho (*8*) was to replace the single slit at the analyzer exit with a detector array. Signal is gained in direct proportion to the number of detectors employed. Note that the final spectrometer resolution is related to the spatial spread of the peaks at the exit plane. This is determined both by the energy spread of the beam incident on the sample and by the resolving power of the analyzer:

$$E/\Delta E \cong \text{sector radius/slit width}$$

In the dispersion-compensation technique (Fig. 1b), there is no exit slit after the monochromator so that the energy spread of the filament is dispersed across the sample. The sample is located at the focus points of both the monochromator and the analyzer. The analyzer now performs two functions. In the instrument configuration shown in Fig. 1b, the analyzer works partly like a monochromator in reverse (these devices are equivalent in the forward and backward directions). It therefore focuses the spatial spread established by the monochromator at the sample to a single point at the exit plane of the analyzer. At the same time, it spatially disperses the energy spread of the electrons scattered inelastically from the surface. Therefore, the fraction of the entire incident energy distribution that is shifted by a constant amount, $-h\nu$ (where $h$ is Planck's constant and $\nu$ is the vibrational frequency of the species excited on the surface), will be focused to a single point at the analyzer exit plane, but it will be displaced by a constant amount from where the elastic beam is focused.

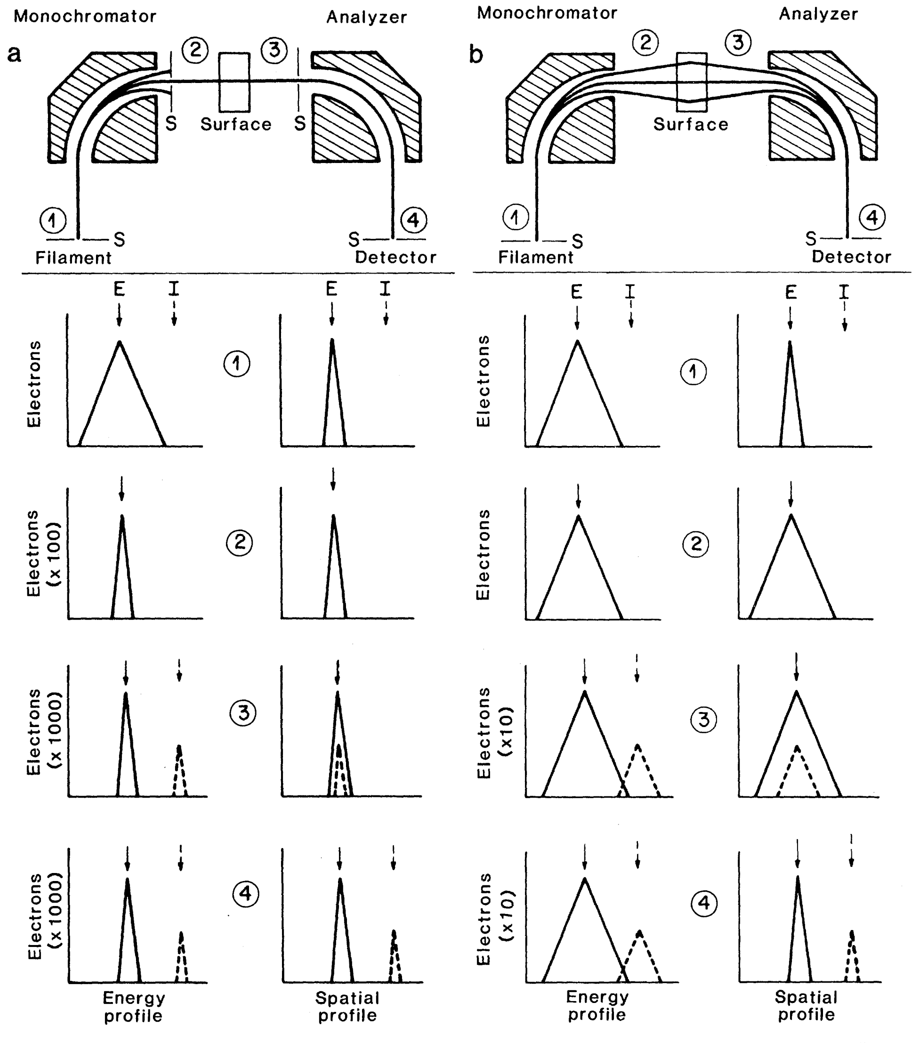

Fig. 1. Schematic diagrams of (a) a conventional high-resolution EELS system and (b) a spectrometer based on the principle of dispersion compensation (*7*). The lower panels show both the energy and the spatial profiles of the electron beam at the four numbered points along its path: (1) monochromator entrance, (2) monochromator exit, (3) analyzer entrance, and (4) detector. The peaks labeled "E" and "I" refer to elastically and inelastically scattered electrons, respectively. The scale changes along the vertical axis as the electrons traverse the spectrometer. The losses are due both to the slits (s) and to the low reflectivity of most samples. The dispersion compensation design greatly enhances the signal level, which is proportional to the square of the energy spread, but does not degrade the resolution, which is proportional to the spatial spread.

Spectra are recorded simply by scanning the analyzer pass energy. The final energy resolution is determined only by the spatial spread at the exit plane. This is related to instrumental considerations (slit and sector sizes) and, to the first order, is independent of the energy spread at the sample. Thus, the spectrometer can be designed to have a resolution comparable to that of conventional EELS instruments but, because of the larger energy spread of the incident beam, a greatly enhanced intensity. The maximum intensity is limited by space-charge effects and is proportional to the square of the energy spread at the sample.

In summary, the EELS experiment is being performed at many energies simultaneously. The dispersion-compensation technique disperses the electrons of each incident energy to a separate part of the surface. At each point an EELS experiment is performed with an elastic peak of different but well-defined absolute energy. In effect, this technique adds all of these spectra together at the output of the analyzer by focusing each elastic peak to the same point in space, independent of its absolute energy.

In an attempt to demonstrate the capabilities of dispersion compensation in EELS instrumentation, a prototype was constructed that is essentially a realization of the schematic in Fig. 1b, with a total scattering angle of 120°. To control second-order aberrations, a premonochromator was installed before the monochromator entrance slit to provide a source that is more well defined energetically. As the preliminary results discussed below demonstrate, the prototype has been a success. Signal intensities are routinely two orders of magnitude greater than those attained with conventional designs.

## Experimental Results and Discussion

Clearly, the improvement made to EELS through the use of the dispersion compensation technique is the large enhancement of the signal at a given loss energy. In practice, elastic peak-count rates in excess of $10^8$ $sec^{-1}$ have been obtained from clean Cu(100) and Ni(111) surfaces, and rates greater than $10^6$ $sec^{-1}$ from the CO stretching mode on these surfaces (*7, 24*). The measured resolution is 12 millielectron volts (meV) [full width at half maximum (fwhm) of the elastic peak], although in principle the design resolution is slightly better than this. By comparison, typical signal counts in a conventional EELS system are $2 \times 10^5$ to $5 \times 10^5$ $sec^{-1}$ in the elastic peak, with no more than $10^4$ $sec^{-1}$ in a loss peak. The resolution generally varies between 4 and 10 meV (fwhm) (*3*).

The ultimate time resolution of this apparatus depends both on the number of loss energies that need to be scanned to make a measurement and on the intensity of each energy-loss peak. Figure 2, for example, shows a series of EELS spectra of a surface formate species on Cu(100), indicating that only three relatively intense modes need to be studied to identify this species (*25*). The signal-to-noise ratio obtained at a measurement rate of 1 to 10 msec per loss energy is high enough that an entire 100-point spectrum can be recorded in 100 msec. For experiments in which the intensity of a single peak provides sufficient information (for example, coverage), a time resolution of 1 msec is possible in a single, nonrepetitive experiment. If the experiment can be repeated, faster time scales or lower coverages can be explored by using signal averaging.

Following is a discussion of three experiments that illustrate different ways of using this improved EELS time resolution. In the case of formic acid adsorbed on Cu(100), the ability to record spectra while dosing, heating, or cooling a sample on reasonable time scales was used to study the orientation of a surface formate species (*26*). In the second example, a result from Ho and his colleagues (*8, 27*) is presented which illustrates how the combination of temperature-programmed desorption (TPD) with TREELS provides a detailed description of the dissociation kinetics of methanol ($CH_3OH$) on Ni(110). Finally, the third example is a direct measurement of the mean residence time and thereby the desorption kinetics of CO on Cu(100) using a combination of TREELS and a pulsed molecular beam (*28*).

*Orientation of the surface formate species on Cu(100) (26).* On most metal and metal-oxide surfaces, the dissociation of formic acid (HCOOH) proceeds by the formation of a surface formate species. This species is stable over a fairly wide temperature range (*29–31*). In many cases, EELS studies have shown that the formate is tilted (that is, has nonequivalent O–Cu bonds) at low temperature (*25, 32, 33*) but is aligned along the surface normal (has equivalent O–Cu bonds) at higher temperatures (*25, 26, 29–35*). These observations were made by dosing either a clean or an oxygen-covered surface with formic acid at low temperature and then annealing to various temperatures. The tilting transition has been suggested to be reversible on Cu(100) (*25, 34*). In those studies the aligned formate was observed to return to the tilted conformation after cooling and waiting for approximately 20 minutes.

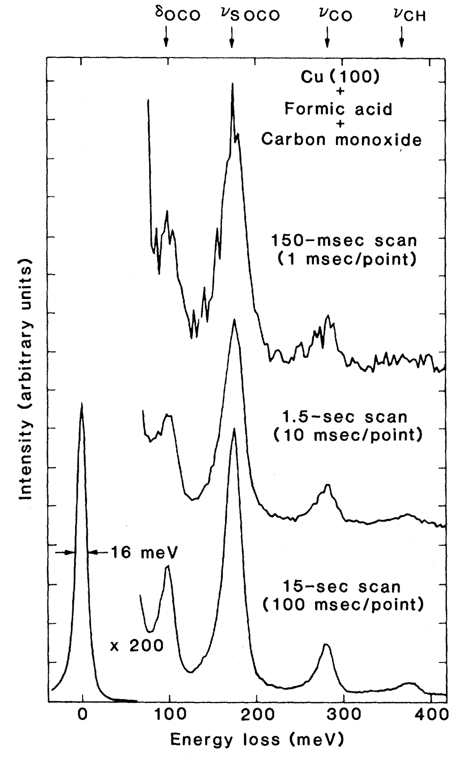

Fig. 2. High-resolution EELS spectra of a mixed layer of surface formate (from the decomposition of formic acid) and adsorbed CO on a Cu(100) single-crystal surface. Spectra were run at three different scan rates to demonstrate the ability of the dispersion-compensation technique (Fig. 1b) (*7*) to measure surface vibrational spectra with a high signal-to-noise ratio under transient conditions. None of these spectra have been signal-averaged or smoothed. The elastic peak (lower left) has a full width at half maximum of 16 meV, and the scale is expanded 200 times so that the energy loss spectrum can be observed. Mode assignments are listed at the top of the figure.

We have studied these orientation effects with TREELS by making measurements dynamically while heating, cooling, and dosing the sample (*26*). We find that the tilting is in fact not reversible under ultrahigh-vacuum conditions; tilting can be obtained only by re-dosing the crystal with formic acid while cooling, and the rate of tilting increases with increasing dosing pressure. We note that in the range of $5 \times 10^{-10}$ torr, a surface can be re-dosed with a monolayer of background gas in approximately 30 minutes.

We have also observed that when dosing a clean surface with formic acid, at a temperature where the high-coverage formate is tilted, the first low-coverage formate observed is not tilted. Only at higher coverages does the tilted conformation appear. Although a time resolution of the order of 1 msec was not required for these studies, the ability to record a complete vibrational spectrum every few seconds has allowed us to follow this process in great detail.

A complete study of this system will be published elsewhere (*26*); meanwhile, it is appropriate to state its conclusion that the tilting is in fact a high-coverage phase change. Similar phase changes are also seen for other, longer chain ($C_2$ to $C_6$) acids (*36*).

*Decomposition of $CH_3OH$ on Ni(110) (8, 27).* The TREELS apparatus designed by Ho and his colleagues (*8, 27*) uses parallel detection at the output to record up to 96 loss energies simultaneously. Although this approach alone does not improve the signal rate for any specific loss event, it does provide a real time observation of the interconversion of chemical species on a surface as a chemical process occurs.

This technique was successfully applied to the study of $CH_3OH$ decomposition on Ni(110). In Fig. 3, we reproduce results from this study. After a $CH_3OH$ dose at low temperature, the surface temperature was increased linearly at a rate of 0.73 K per second; the adsorbate subsequently decomposed with the eventual desorption of products. The temporal development of the adsorbed species was followed with the parallel processing EELS spectrometer, whereas the desorption products were detected with a mass spectrometer.

On the basis of the observed decay of

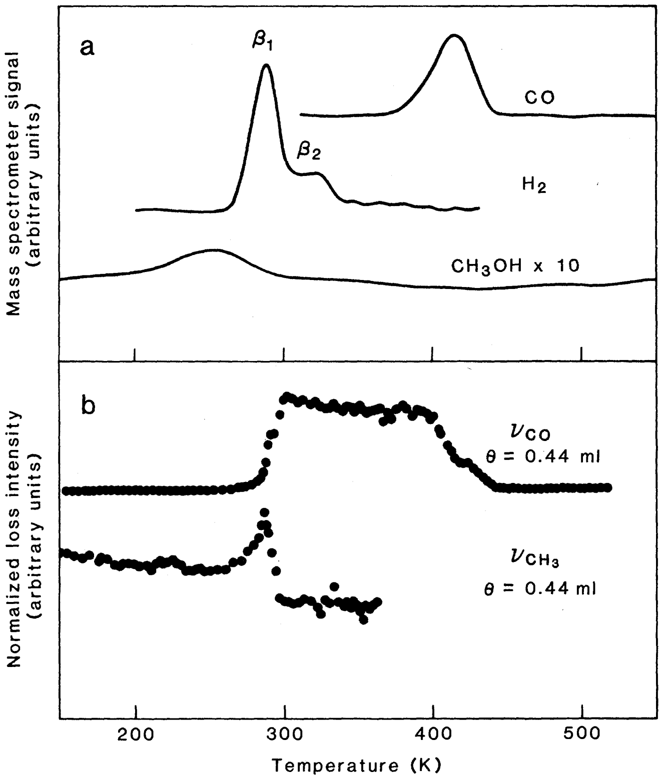

Fig. 3. Results from the studies by Richter et al. (*27*) of the decomposition of $CH_3OH$ on Ni(110) with (a) TPD and (b) temperature-programmed EELS. The value of $\nu_{CO}$ is 238 meV, and the value of $\nu_{CH_3}$ is 362 meV. The sample was dosed with a saturation overlayer at 170K and heated linearly at a rate of 0.73 K per second. [Courtesy of Elsevier]

the $CH_3$ stretching mode from an adsorbed methoxide ($CH_3O$) intermediate and the subsequent appearance of adsorbed CO and desorbed $H_2$, a mechanism for the decomposition was proposed that included stepwise removal of hydrogen from $CH_3O$, with abstraction of the first hydrogen being the rate-limiting step. A quantitative measure of the reaction rate constant was obtained by varying both the heating rate and the initial surface coverage. TREELS and TPD are clearly a powerful combination for the elucidation of simple surface reaction mechanisms.

*Adsorption and desorption kinetics of CO and Cu(100) (28).* The direct, real-time measurement of a surface rate process in the millisecond time range is the goal of TREELS experiments. We have now measured the transient signal from adsorbed CO on Cu(100) following pulsed dosing of the surface at low temperature. Analysis of the decay of the surface CO population gives the desorption rate constant, which can be measured as a function of both surface temperature and coverage. In this system the loss of energy is known to be independent of coverage, and the loss intensity is linearly related to coverage over a wide range (*37, 38*).

We have confirmed that this is also the case in our spectrometer. We obtained a linear intensity increase at constant dosing pressure when we normalized the loss intensity either to the elastic peak or to the background level. In general, however, it will be necessary to account for nonlinearities by careful normalization of peak intensities and of positions as a function of coverage.

To measure accurate desorption kinetics, a well-resolved time event must be created at the surface. In our studies this is accomplished by starting with a clean copper surface at a given temperature and exposing it to a pulsed dose of carbon monoxide. When the surface is held at a temperature at which the mean residence time is greater than a few milliseconds, the time evolution of the surface coverage can be measured. To achieve the fastest time resolution, the spectrometer is tuned to the peak of the C–O stretching vibration. To further improve the signal-to-noise ratio, the pulsed dose can be cycled many times. Since the pulse shape of the incoming dose is known, the resulting signal-averaged waveform (surface coverage versus time) can be deconvoluted to yield the desorption rate constant.

Figure 4 shows both experimental and theoretical waveforms for three values of the copper substrate temperature. As the surface temperature is increased, the CO residence time decreases, as shown by the faster decay of the adsorbate surface coverage. The desorption rate constant is derived from the data by assuming first order kinetics:

$$\dot{n}(t) = SI(t) - k_d n(t) \qquad (1)$$

where $S$ is the sticking coefficient, $I(t)$ is the incident flux, $k_d$ is the desorption rate constant, and $n(t)$ is the time-dependent surface population. Our present pulsed doser has a very sharp rise time followed by a long exponential tail so that

$$I(t) = I_0 e^{-\lambda t} \qquad (2)$$

where $1/\lambda \approx 150$ msec. This results in the following waveform:

$$n(t) = \frac{SI_0}{k_d - \lambda}[e^{-\lambda t} - e^{-k_d t}] \qquad (3)$$

The first-order desorption rate constant, $k_d$, was obtained by fitting Eq. 3 to the experimental data at each surface temperature. The temperature dependence of the desorption rate constants so obtained yields an activation energy and preexponential factor that are consistent with known values (*39*). The CO on Cu(100) system was chosen for these first measurements because of its simplicity, and therefore the information obtained so far is not beyond the capabilities of equilibrium measurements. The success of these first measurements, however, indicates the possibilities for measurements of more complex systems in which there are multiple binding sites or in which reactions occur. For many of these cases, direct real-time studies will be able to isolate individual reaction steps that otherwise would be inaccessible to measurement. In future experiments the doser will be replaced by a differentially pumped molecular beam to obtain narrower pulses, which will extend the measuring range to faster kinetics and improve accuracy.

A significant advantage provided by the direct measurement of the surface-coverage waveform (rather than measurement of the scattered-flux waveform) is that the absolute surface coverage is known. This is because EELS intensities are often linearly proportional to coverage, particularly at low adsorbate coverage (*3*). In addition, the maximum coverage in the data shown in Fig. 4 is 4 percent of a monolayer (upper trace), and we have the sensitivity to measure peak coverages of less than 0.5 percent (lower trace). This high sensitivity makes it possible to study the coverage dependence of adsorption and desorption kinetics. This can be done by using a constant beam to establish an initial fixed coverage [$n(t)$ = constant] and then using the pulsed beam to provide a small increase in that coverage. The resulting waveform is characteristic of the kinetics at the initial coverage. A final advantage of this technique is that the normalization of peak intensities is simple, since any changes in spectrometer performance are expected to be small over the small changes in surface coverage probed.

Another application that makes use of the extreme sensitivity of this apparatus is to explore changes in kinetics that have been observed at very low coverages. It has been shown (*13*) that surface steps and surface defects may control the kinetics in this regime because the first molecules that reach the surface will diffuse quickly to the strongest binding sites. We have some experimental evidence that suggests that the kinetics of desorption of CO from copper are significantly perturbed when these sites are blocked (*28*). Such coverage-dependent studies are generally more difficult and less direct when using desorption techniques than when using the TREELS techniques involved in Fig. 4.

## Conclusions

Two recent improvements in EELS instrumentation [dispersion compensation (*7*) and parallel detection (*8*)] have been shown to improve the time resolution of the EELS technique by several orders of magnitude. The prototype apparatuses that first incorporated these innovations have been used to improve the time resolution in studies of a variety of surface dynamic processes (*8, 26–28, 40*). New spectrometers that incorporate further improvements are now being designed and built. One goal is to obtain resolution at least as good as that obtained in conventional high-resolution EELS; achieving this goal would, in itself, greatly enhance the versatility of EELS.

The most important development has been the ability to make real-time measurements of surface rate processes. We are presently constructing a spectrometer that will combine dispersion compensation with parallel detection to provide both fast-time resolution and chemical sensitivity simultaneously. (The feasibility of this combination is indicated in Fig. 1b.) In addition, improvements in the electron optics should provide even more intensity, better resolution, and reduced background noise. The spectrometer will be combined with a high-intensity molecular beam source and a mass spectrometer to detect scattered and desorbed molecules.

The key to understanding surface rate processes is the ability to follow them from beginning to end. This means that (i) well-defined reactants must be prepared and delivered to the surface, (ii) the process must be monitored in real time at the surface, and (iii) any gaseous products must be detected after desorption. Molecular beam techniques have been refined to the point where the first step is possible, and the detection of gaseous products is now well defined for both mass spectrometers (to provide chemical and kinetic energy information) and lasers (to provide internal state information). Until now, however, the lack of experimental probes with sufficient dynamic range has meant that the second step, which is what one wants to measure, has been a "black box." TREELS is the first technique capable of following the complete cycle of a surface rate process. This will greatly improve our understanding of surface kinetics, an area that is both fundamentally and technologically important.

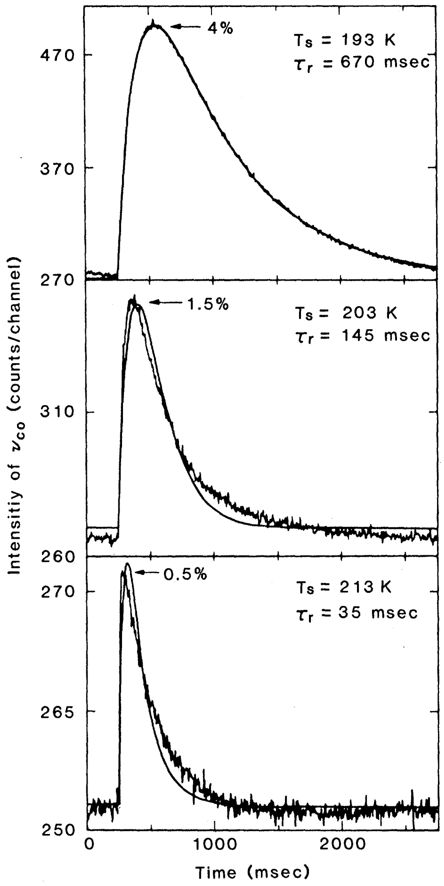

Fig. 4. Experimental and theoretical (solid line) waveforms recorded while dosing a clean Cu(100) surface with a pulsed molecular beam of carbon monoxide approximately 150 msec wide. Increasing surface temperature ($T_s$) clearly decreases both the maximum CO coverage and residence time ($\tau_r$). The vertical scale indicates the number of counts per channel (each channel is 5 msec wide). The relatively high background level will be removed by future spectrometers. The top two traces are averages of 200 pulses while the lower trace is the average of 600 pulses.

### References and Notes

1. G. A. Somorjai and M. A. Van Hove, *Structure and Bonding* (Springer-Verlag, New York, 1978), vol. 38.
2. E. W. Plummer and W. Eberhardt, *Advances in Chemical Physics* (Wiley, New York, 1982), vol. 49.
3. H. Ibach and D. L. Mills, *Electron Energy Loss Spectroscopy and Surface Vibrations* (Academic Press, New York, 1982).
4. R. J. Madix and J. Benziger, *Ann. Rev. Phys. Chem.* **29**, 285 (1978).
5. M. J. Cardillo, *ibid.* **32**, 332 (1982).
6. J. C. Tully, *ibid.* **31**, 319 (1982).
7. S. D. Kevan and L. H. Dubois, *Rev. Sci. Instrum.* **55**, 1604 (1984).
8. W. Ho, *J. Vac. Sci. Technol.* **A3**, 1432 (1985).
9. J. B. Taylor and I. Langmuir, *Phys. Rev.* **44**, 423 (1933).
10. P. J. Kisliuk, *J. Phys. Chem. Solids* **3**, 95 (1957).
11. D. A. King and M. G. Wells, *Proc. R. Soc. London Ser. A* **339**, 245 (1974).
12. M. J. Grunze *et al.*, *Surf. Sci.* **139**, 109 (1984).
13. J. A. Serri, M. J. Cardillo, G. E. Becker, *J. Chem. Phys.* **77**, 2175 (1982); J. A. Serri, J. C. Tully, M. J. Cardillo, *ibid.* **79**, 1530 (1983).
14. R. J. Madix, in *The Chemical Physics of Solid Surfaces*, D. A. King and D. P. Woodruff, Eds. (Elsevier, New York, 1982), vol. 4, p. 1.
15. O. K. Rice and H. C. Ramsperger, *J. Am. Chem. Soc.* **49**, 1617 (1927); *ibid.* **50**, 617 (1928); O. K. Rice, *Proc. Natl. Acad. Sci. U.S.A.* **14**, 114 (1928).
16. L. S. Kassel, *Kinetics of Homogeneous Gas Reactions* (Van Nostrand, New York, 1982).
17. E. T. Foxon and B. A. Joyce, *Surf. Sci.* **64**, 293 (1977).
18. J. R. Arthur, *J. Appl. Phys.* **39**, 4032 (1968).
19. D. P. Dapkas, *Annu. Rev. Mater. Sci.* **12**, 243 (1982).
20. A. Y. Cho, *Thin Solid Films* **100**, 291 (1983).
21. G. Herzberg, *Molecular Spectra and Molecular Structure* (Van Nostrand, New York, 1945), vol. 2.
22. S. D. Kevan, *Rev. Sci. Instrum.* **54**, 1441 (1983).
23. J. E. Pollard *et al.*, *ibid.* **52**, 1837 (1981).
24. L. H. Dubois, T. H. Ellis, S. D. Kevan, *J. Vac. Sci. Technol.* **A3**, 1643 (1985).
25. B. A. Sexton, *Surf. Sci.* **88**, 319 (1979).
26. L. H. Dubois, T. H. Ellis, B. R. Zegarski, S. D. Kevan, in preparation.
27. L. J. Richter *et al.*, *Chem. Phys. Lett.* **111**, 185 (1984); L. J. Richter and W. Ho, *J. Vac. Sci. Technol.* **A3**, 1549 (1985).
28. T. H. Ellis, L. H. Dubois, S. D. Kevan, M. J. Cardillo, in preparation.
29. D. H. S. Ying and R. J. Madix, *J. Catal.* **61**, 48 (1980).
30. M. Bowker and R. J. Madix, *Surf. Sci.* **102**, 542 (1981).
31. B. E. Hayden, K. Prince, D. P. Woodruff, A. M. Bradshaw, *ibid.* **133**, 589 (1983).
32. B. A. Sexton and R. J. Madix, *ibid.* **105**, 177 (1981).
33. S. L. Miles, S. L. Bernasek, J. L. Gland, *ibid.* **127**, 271 (1983).
34. P. Hofmann, C. Mariani, K. Horn, A. M. Bradshaw, *Vide* **201** (suppl., vol. 1), 541 (1980).
35. J. Stöhr, D. A. Outka, R. J. Madix, U. Döbler, *Phys. Rev. Lett.* **54**, 1256 (1985).
36. L. H. Dubois, B. R. Zegarski, R. G. Nuzzo, in preparation.
37. B. A. Sexton, *Chem. Phys. Lett.* **63**, 451 (1979).
38. S. Andersson, *Surf. Sci.* **89**, 477 (1979).
39. J. C. Tracy, *J. Chem. Phys.* **56**, 2748 (1972).
40. B. A. Gurney and W. Ho, *J. Vac. Sci. Technol.* **A3**, 1541 (1985).

41. We thank J. C. Tully for providing insight and assisting with the modeling.